Biogeosciences, 9, 2385–2399, 2012
www.biogeosciences.net/9/2385/2012/
doi:10.5194/bg-9-2385-2012

Biogeosciences

Use of the isotope flux ratio approach to investigate the $C^{18}O^{16}O$ and $^{13}CO_2$ exchange near the floor of a temperate deciduous forest

E. Santos[1], **C. Wagner-Riddle**[2], **X. Lee**[3], **J. Warland**[2], **S. Brown**[2], **R. Staebler**[4], **P. Bartlett**[5], **and K. Kim**[3]

[1]Department of Agricultural Engeneering, Federal University of Viçosa, Viçosa, MG, Brazil
[2]School of Environmental Sciences, University of Guelph, Guelph, ON, N1G 2W1, Canada
[3]School of Forestry and Environmental Studies, Yale University, New Haven, CT, USA
[4]Climate Processes Section, Environment Canada, Toronto, ON, Canada
[5]Air Quality Processes Research Section, Environment Canada, Toronto, ON, Canada

Correspondence to: C. Wagner-Riddle (cwagnerr@uoguelph.ca)

Received: 29 June 2011 – Published in Biogeosciences Discuss.: 1 August 2011
Revised: 24 April 2012 – Accepted: 29 April 2012 – Published: 2 July 2012

Abstract. Stable isotopologues of CO_2, such as $^{13}CO_2$ and $C^{18}OO$, have been used to study the CO_2 exchange between land and atmosphere. The advent of new measuring techniques has allowed near-continuous measurements of stable isotopes in the air. These measurements can be used with micrometeorological techniques, providing new tools to investigate the isotope exchange in ecosystems. The objectives of this study were to evaluate the use of the isotope flux ratio method (IFR) near the forest floor of a temperate deciduous forest and to study the temporal dynamics of $\delta^{18}O$ of CO_2 flux near the forest floor by comparing IFR estimates with estimates of $\delta^{18}O$ of net soil CO_2 flux provided by an analytical model. Mixing ratios of $^{12}C^{16}O_2$, $^{13}CO_2$ and $C^{16}O^{18}O$ were measured within and above a temperate deciduous forest, using the tunable diode laser spectroscopy technique. The half-hourly compositions of the CO_2 flux near the forest floor ($\delta^{13}C_F$ and $\delta^{18}O_F$) were calculated by IFR and compared with estimates provided by a modified Keeling plot technique (mKP) and by a Lagrangian dispersion analysis (WT analysis). The mKP and IFR $\delta^{18}O_F$ estimates showed good agreement (slope = 1.03 and correlation, R^2 = 0.80). The $\delta^{13}C_F$ estimates from the two methods varied in a narrow range of −32.7 and −23.1 ‰; the mean (± SE) mKP and IFR $\delta^{13}C_F$ values were −27.5 ‰ (±0.2) and −27.3 ‰ (±0.1), respectively, and were statistically identical ($p > 0.05$). WT analysis and IFR $\delta^{18}O_F$ estimates showed better correlation (R^2 = 0.37) when only turbulent periods ($u_* > 0.6\,\mathrm{m\,s^{-1}}$) were included in the analysis. The large amount of data captured (∼95 % of half-hour periods evaluated) for the IFR in comparison with mKP (27 %) shows that the former provides new opportunities for studying $\delta^{18}O_F$ dynamics within forest canopies. Values of $\delta^{18}O_F$ showed large temporal variation, with values ranging from −31.4 ‰ (DOY 208) to −11.2 ‰ (DOY 221). Precipitation events caused substantial variation (∼8 ‰) in $\delta^{18}O_F$ over a period of approximately 24 h. A diel trend of $\delta^{18}O_F$ was observed, with more depleted values present during the daytime. Model simulations indicate that the activity of the carbonic anhydrase enzyme was quite variable during the evaluated period. These simulations indicate that more frequent sampling of $\delta^{18}O$ of soil water could improve the estimates of $\delta^{18}O$ of net soil CO_2 flux.

1 Introduction

Stable isotopes of CO_2 have been used to investigate the exchange of carbon dioxide between land and atmosphere (Keeling, 1958; Farquhar et al., 1993; Ciais et al., 1995; Yakir and Wang, 1996; Cuntz et al., 2003). Naturally occurring CO_2 isotopologues, such as $^{13}CO_2$ and $C^{18}OO$, have been used to study the uptake of CO_2 by oceans and land (Tans et al., 1993; Ciais et al., 1995), to investigate the exchange of CO_2 between ecosystems and atmosphere and for partitioning the net CO_2 ecosystem exchange into photosynthetic and respiratory fluxes (Yakir and Wang, 1996; Bowling et al., 2001; Ogée et al., 2004; Zhang et al., 2006).

The isotopologue $^{13}CO_2$ has been used as a tracer in ecosystems where there is a contrast between the isotope compositions ($\delta^{13}C$) of growing plants and soil organic matter (Rochette et al., 1999; Griffis et al., 2005b). This contrast is commonly observed either when C_3 plants are growing in soil with organic carbon derived from C_4 residue or vice versa, and it is caused by differences in the photosynthetic isotopic discrimination between C_3 and C_4 plants (Farquhar et al., 1989). On the other hand, the use of $C^{18}OO$ as a tracer relies on differences in ^{18}O composition ($\delta^{18}O$) of CO_2 fluxes originating from soil and plant canopies (Gillon and Yakir, 2001). The $\delta^{18}O$ of canopy and soil CO_2 fluxes is coupled with $\delta^{18}O$ of soil and leaf water. Differences in $\delta^{18}O$ between soil and foliage water pools arise as $H_2^{16}O$ evaporates more readily than $H_2^{18}O$ and due to different evaporation rates between water pools (Farquhar and Cernusak, 2005; Welp et al., 2008). Ogée et al. (2004) proposed the use of carbon and oxygen isotope tracers for partitioning the net CO_2 ecosystem exchange into plant and soil components. The use of $C^{18}OO$ is particularly advantageous in established ecosystems where the $\delta^{13}C$ differences between plants and soil organic matter are not very large (Ogée et al., 2004; Griffis et al., 2005a).

One of main challenges of using $C^{18}OO$ as a tracer in ecosystems is its large temporal dynamics (Griffis et al., 2005a; Wingate et al., 2010; Xiao et al., 2010), which is controlled by variables such as changes in environmental conditions, efficiency of the CO_2 hydration, kinetic fractionation, isotopic composition of water in the soil and foliage (Yakir and Sternberg, 2000; Seibt et al., 2006). Seibt et al.(2006) observed that the rate of equilibration between CO_2 and water in soils could not be explained strictly by soil physical properties and hypothesized that the rate of CO_2 hydration was enhanced by the activity of carbonic anhydrase enzyme (CA) in the soil. Soil chamber studies have shown that the effect of CA varies in time and between sites, so additional studies are required to quantify the level of activity of the CA in the soil in different biomes (Seibt et al., 2006; Wingate et al., 2008, 2010). Furthermore, chamber studies have brought new insights into mechanisms controlling the $C^{18}O^{16}O$ exchange in soils; however, the use of soil chambers in ecosystem-scale studies requires a very intensive sampling scheme to characterize the spatial heterogeneity of ecosystem fluxes (Law et al., 1999; Davidson et al., 2002; Powers et al., 2010). In addition, soil chambers can significantly affect the $C^{18}OO$ exchange between soil and air, requiring the use of soil diffusion models to correct for this effect (Seibt et al., 2006).

The advent of new measuring techniques, such as quantum cascade laser-based spectrometry (Tuzson et al., 2008; Kammer et al., 2011) and tunable diode laser absorption spectroscopy (Bowling et al., 2003b; Griffis et al., 2005a, 2008; Wingate et al., 2010), has allowed near-continuous measurements of CO_2 isotopologues in the air. These measurements can be combined with existing micrometeorological techniques, allowing the investigation of isotope exchange in spatial and temporal scales suitable for studying ecosystem biophysical processes (Griffis et al., 2007; 2010). Griffis et al. (2004) proposed the use of the isotope flux ratio method (IFR), based on gradient-diffusion theory, to determine the isotope composition of ecosystem respiration. This approach shows some advantages over the commonly used Keeling plot technique (KP) (Keeling, 1958), since it is theoretically less sensitive to changes in background atmospheric CO_2 mixing ratios and provides estimates of flux components that are consistent with the flux footprint (Griffis et al., 2004, 2007). The IFR method could be particularly helpful to study $C^{18}OO$ exchange since the conventional KP technique, with concentration data collected during large time intervals (several hours), is not as reliable for determining the ^{18}O composition of fluxes as when applied to ^{13}C measurements (Tans, 1998; Flanagan et al., 1999; Griffis et al., 2005a).The IFR method has been applied to investigate the isotope exchange above plant canopies. Studies have shown that the gradient-diffusion theory, in principle, is not suitable to study mass and energy exchange within plant canopies, due to the close proximity of sources/sinks and to the length scale of turbulent eddies inside plant canopies (Corrsin, 1974; Denmead and Bradley, 1987). However, it has been shown that the gradient-diffusion based approaches provide reasonable estimates of fluxes in the open trunk space of forests (Dolman and Wallace, 1991; Baldocchi and Meyers, 1991; Wu et al., 2001). According to the localized near-field theory of Raupach (1989a), a gas constituent that originates from sources at the ground below a vegetation stand can be described by the gradient-diffusion model.

The use of the IFR method beneath plant canopies could bring new insights into mechanisms regulating the isotope exchange in ecosystems. In this study, near-continuous measurements of $^{12}C^{16}O_2$, $^{13}CO_2$ and $C^{18}OO$, obtained using tunable diode laser absorption spectroscopy, were used for the first time with the IFR approach to study the isotopic exchange near the floor of a temperate deciduous forest. Thus, the objectives of this study were

1. to evaluate the use of the IFR method near the forest floor of a temperate deciduous forest by comparing its estimates of isotope composition of CO_2 flux with values provided by a modified KP technique (mKP) and the analytical Lagrangian dispersion analysis proposed by Warland and Thurtell (2000). The latter analysis takes into consideration the proximity of source and sinks and the length scale of turbulence within plant canopies.

2. to compare the $\delta^{18}O$ of CO_2 flux measured using the IFR near the forest floor with modeled $\delta^{18}O$ of soil CO_2 flux obtained using an analytical model (Tans, 1998; Amundson et al., 1998; Wingate et al., 2009). This model has been tested in chamber-based studies and can be used to investigate the effect of environmental variables, such as the isotope composition of precipitation

Table 1. Textural composition and organic carbon content of the soil in a deciduous forest.

Depth (cm)	Texture (%)*			C (%)**
	Sand	Silt	Clay	
0–10	87.1 (±3.6)	8.2 (±2.6)	4.6 (±1.1)	2.40 (±0.03)
10–15	90.5 (±0.6)	6.5 (±0.8)	3.0 (±0.6)	0.66 (±0.03)
15–30	95.1 (±1.0)	3.3 (±1.3)	1.6 (±0.4)	0.63 (±0.02)
30–45	95.3 (±1.4)	3.3 (±1.3)	1.3 (±0.6)	0.53 (±0.02)
45–60	96.8 (±1.3)	2.4 (±1.1)	0.8 (±0.4)	0.52 (±0.02)

* soil texture analysis was obtained from three soil cores. Numbers in brackets are ±1 standard deviation
** soil carbon content from nine soil cores.

and the activity of soil CA on the temporal dynamics of $\delta^{18}O$ of CO_2 flux near the forest floor (Wingate et al., 2010).

2 Materials and methods

2.1 Site description

The experiment was carried out in a deciduous forest at the Environment Canada research station at Borden, ON, Canada (44°19′ N, 79°56′ W) from June to September 2009. The approximately 100-year-old forest, consisting of natural re-growth on abandoned farmland, is composed of mixed hardwood and coniferous species (Neumann and den Hartog, 1989). A survey conducted in 2006 indicates that red maple (*Acer rubrum* L.) is the predominant tree species (52.2 %) followed by eastern white pine (*Pinus strobus* L.) with 13.5 %, and large-tooth aspen (*Populus grandidentata* Michx.) and white ash (*Fraxinus americana* L.) (∼7 % each) (Teklemariam et al., 2009). In July 2009, the stand height was approximately 22 m and the leaf area index (±SE) was 3.9 (±0.13) $m^2\ m^{-2}$.

The terrain at the site presents variations of elevation within 2 m, except for a 20-m deep and 40-m wide river valley located 1 km south from the 44 m sampling tower and a 6-km wide swamp located 5 km northeast from the tower (Lee et al., 1999). Textural analysis of soil cores indicated loamy sand soil at the site and an increase in the proportion of sand in the soil with depth (Table 1). The averaged carbon content was equal to 2.4 % by mass in the 0–10 cm layer.

2.2 Measurements of mixing ratios of stable isotopes of carbon dioxide

Mixing ratios of the isotopologues, $^{12}C^{16}O_2$, $^{13}CO_2$ and $C^{18}OO$, were measured at 10 Hz within the forest canopy and above the forest using a sampling system connected to a tunable diode laser trace gas analyzer (TGA100A, Campbell Scientific, Logan, UT, USA; hereafter TGA), kept in a temperature-controlled enclosure set up in a trailer. The TGA measures the mixing ratio of trace gases in the air by comparing the infrared absorption of sample and reference gas in a specific absorption line of the spectrum. Additional details about stable isotope measurements using the TGA can be found elsewhere (Bowling et al., 2003b; Lee et al., 2005; Griffis et al., 2005a). The air was sampled using eight air intakes, set up within and above the forest canopy at 0.45, 1.45, 5.51, 9.65, 16.69, 20.77, 25.81 and 36.81 m (Fig. 1). In the first stage of the experiment (day of year, DOY = 182 to 229), only the two closest intakes to the forest floor were sampled during weekends. On week days (Monday to Friday) measurements were taken above the forest; results related to these measurements will be presented in a future study. From DOY 237 to 260, all eight air intakes were sampled.

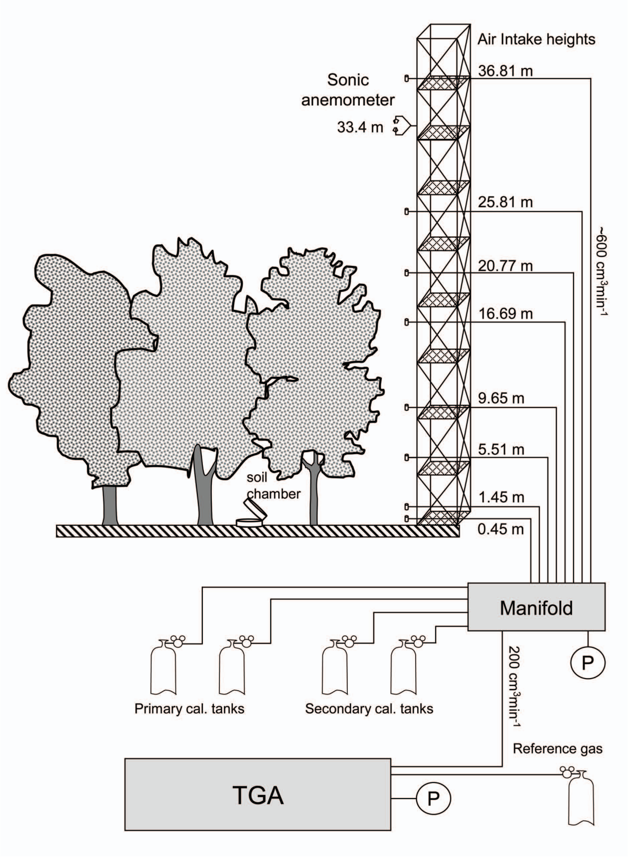

Fig. 1. Experimental setup used to study $C^{16}O_2$ and $C^{18}OO$ exchange in a temperate deciduous forest in Borden, ON, Canada. TGA denotes tunable diode laser; P shows placement of vacuum pumps. Placements of the automatic soil chamber used to measure the soil CO_2 flux and sonic anemometer are also shown.

Each air intake consisted of a 1 m stainless tube (0.43 cm I.D.) with a rain diverter and mesh screen in one of its extremities. The other extremity of the tube was connected to a stainless filter (SS-4F-K4-7, 7 µm sintered element filter, Swagelok, OH, USA). In order to prevent condensation, the filter holder was heated using a 0.5 W heater

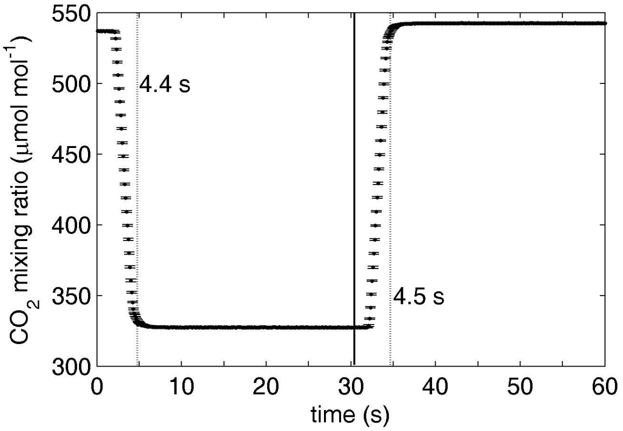

Fig. 2. Average $^{12}C^{16}O_2$ mixing ratios (±1 standard deviation) measured during switching between secondary calibration standards at 10 Hz ($n = 44$). The solid horizontal lines indicate the times (0 and 30 s) when the TGA sampling system switched from low (327 μmol mol^{-1}) to high (∼543 μmol mol^{-1}) concentration calibration tanks, and dotted lines indicate the times (4.4 and 4.5 s) after switching air intakes at which TGA readings reached 95 % of the total response.

connected to a 12 V DC power supply and a critical flow orifice located downstream of the filter was used to reduce the air pressure in the intake line. Approximately 40 m of polyethylene/aluminum tube (0.43 I.D., Synflex 1300, Aurora, OH, USA) directed the sample to a custom-made manifold (Campbell Scientific).

The manifold was used to control the flow of ambient air from the air inlets and calibration gases through the TGA. The duration of each sampling cycle was 5 min, in which the system measured atmospheric and secondary calibration tank mixing ratios for each isotopologue. The sampling system manifold switched between air intakes every 15 s for 4 min, and then each of the two calibration tanks was sampled for 30 s. The air was pulled continuously through all air intakes at a flow rate of approximately 600 cm^3 min^{-1} using a vacuum pump (RB0040, Bush Vac. Tec., Boisbriand, QC, Canada). A sub-sample of the total flow was directed to the TGA at a flow rate of 200 cm^3 min^{-1} in order to maintain the TGA sample cell at approximately 1.8 kPa reducing the pressure broadening of the absorption line (Bowling et al., 2003b).

The secondary calibration tanks were compared weekly with two primary calibration standards obtained from the Stable Isotope Laboratory (SIL) at the Institute of Arctic and Alpine Research, University of Colorado, in cooperation with the Earth System Research Laboratory (ESRL/GMD) of the National Oceanic and Atmospheric Administration. The calibration values for primary standard A were CO$_2$ mixing ratio = 360.62 μmol mol^{-1}, $\delta^{13}C = -8.475$ ‰ (±0.003 ‰) and $\delta^{18}O = -1.037$ ‰ (±0.006 ‰). Primary standard B consisted of CO$_2$ mixing ratio = 545.77 μmol mol^{-1}, $\delta^{13}C = -16.202$ ‰ (±0.002 ‰) and $\delta^{18}O = -11.861$ ‰ (±0.007 ‰). The calibration of the secondary tanks followed the two point calibration procedure suggested by Bowling et al. (2003b). An example of corrected mixing ratios for secondary tanks and standard deviations, obtained during a weekly calibration, is shown in Table 2.

TGA measurements during tank calibration were also used to determine the time necessary to flush the TGA sampling cell after switching intakes (Fig. 2). The time required for the TGA to reach 95 % of the total response after switching between high (∼545 μmol mol^{-1}) and low (∼330 μmol mol^{-1}) $^{12}C^{16}O_2$ concentration tanks was ∼4.5 s, which was the same time response obtained for $C^{18}OO$ and $^{13}CO_2$. Thus, the mixing ratios of the two isotopologues for each intake and calibration tanks were extracted from the dataset, discarding 5 s after switching intakes. A total of 50 data points were discarded after switching intakes giving a total of 4800 data points per sampled height and 3000 data points per calibration cycle every 30 min when the TGA system was sampling the two intakes near the forest floor. High-frequency sampling (10 Hz) allows for large number of measurements at each observation height and has the advantage of improving the precision of concentration difference measurements (Wagner-Riddle et al., 2005). The data were averaged into 5 min intervals and corrected using the measurements obtained from each calibration tank during each measuring cycle. The corrected data were used to calculate half-hour mean mixing ratios for each isotopologue. The isotope ratios of CO$_2$ in the air ($\delta^{13}C_a$ and $\delta^{18}O_a$) were expressed according to the delta notation, in reference to the Viena Peedee Belemnite (VPDB) scale, i.e. [^{13}C]/[^{12}C] = 0.0111797, which differs from the Chicago Peedee Belemnite ([^{13}C]/[^{12}C] = 0.112372) by approximately 5 ‰, and [^{18}O]/[^{16}O] = 0.002088349077 (Allison et al., 1995; Griffis et al., 2004).

2.3 Supporting measurements

The temporal variation of half-hourly soil CO$_2$ flux was measured using one automated dark chamber (Li-8100, LI-COR) with a 20 cm diameter. Automated chamber measurements (F_{static}) were taken every 15 min and averaged into half-hour intervals. To correct F_{static} for the effect of spatial heterogeneity of the soil flux, the net soil CO$_2$ flux (F_R) was measured weekly using a static chamber at 10 different points in an area adjacent to where the automated measurements were taken. A linear model ($F_R = 0.727 + 0.623F_{\text{static}}$, $R^2 = 0.88$, $p < 0.001$) was used to scale up the single-point soil chamber measurements, following Ohkubo et al. (2007). Measurements of F_R were used for modeling the $\delta^{18}O$ of net soil CO$_2$ flux (see Sect. 2.5).

Soil samples were taken weekly to determine the $\delta^{18}O$ of soil water ($\delta^{18}O_{sw}$) at 5, 10 and 50 cm depth. Liquid water from soil samples was extracted using the cryogenic vacuum extraction method (Ehleringer and Osmond, 1989). In

Table 2. CO_2 isotopologues mixing ratio (± mean standard error) of secondary calibration tanks obtained during weekly calibration on day of year 188.

Tank	Mixing ratio (µmol mol^{-1}) $^{12}CO_2$	$^{13}CO_2$	$C^{18}OO$
1	327.142 (±0.007)	3.4973 (± 0.0001)	1.32671 (±0.00003)
2	542.701 (±0.007)	5.9483 (± 0.0001)	2.22550 (±0.00003)

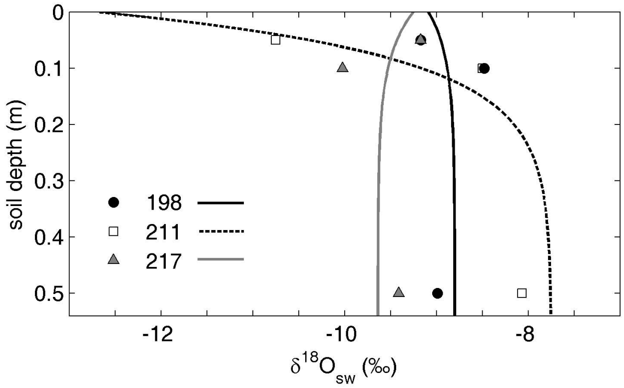

Fig. 3. Measured (symbols) and fitted (lines) profiles of ^{18}O values for soil water ($\delta^{18}O_{sw}$) for three sampling dates (day of year, DOY = 198, 211 and 217) in a temperate deciduous forest. Here $\delta^{18}O_{sw}$ is expressed in the VSMOW scale and was sampled at three depths: 0.05, 0.10 and 0.50 m. Fitted curves are exponential functions with e-foldings of 5 cm (DOY = 198 and 217) and 8 cm (DOY = 211).

addition, the $\delta^{18}O$ of precipitation water ($\delta^{18}O_{pw}$) was determined on an event basis. The precipitation water was collected using a plastic funnel (∼15 cm diameter) placed on the top of a thermally insulated plastic bottle and then stored in sealed glass vials. The $\delta^{18}O$ of soil and precipitation was determined using the CO_2 equilibration method on a gas bench auto sampler attached to a mass spectrometer (Delta Plus XL, Thermo Finnigan, Bremen, Germany) with precision of 0.1 ‰. The $\delta^{18}O$ of soil water and precipitation was expressed relative to the Vienna Standard Mean Ocean Water (VSMOW) in the delta scale. Profiles of $\delta^{18}O_{sw}$, used to model $\delta^{18}O$ of soil CO_2 flux (Sect. 2.5 and Appendix B), were obtained by fitting exponential functions with e-foldings of 5 and 8 cm to measured $\delta^{18}O_{sw}$ (Fig. 3), as proposed by Wingate et al. (2008). The mean absolute difference between measured and estimated $\delta^{18}O_{sw}$ ranged from 0.25 ‰ (DOY 198) to 0.53 ‰ (DOY 211). Lighter $\delta^{18}O_{sw}$ values close to the soil surface on DOY 211 were a result of a precipitation event on DOY 206 with $\delta^{18}O_{sw}$ = –14.64 ‰.

Soil temperature (T_s) and water content (θ_w) were measured at 10 cm depth using thermocouples (105T, Campbell Scientific, Logan, UT, USA.) and moisture probes (CS615-L, Campbell Scientific, Logan, UT, USA), respectively. The precipitation and air temperature were measured in an open pond area adjacent to the site using a tipping bucket rain gauge (Belfort, Baltimore, MD) and air temperature probe (HMP45A, Vaisala, Vantaa, Finland). The wind velocity components were measured at 33.4 m using a sonic anemometer (CSAT3, Campbell Scientific, Logan, UT, USA, Fig. 1).

2.4 Determining the δ^{18}O and δ^{13}C of CO_2 flux near the forest floor

Three methods were used to determine the isotope composition of CO_2 flux near the forest floor: IFR, mKP and WT analysis. Griffis et al. (2004) proposed the gradient diffusion theory to calculate the ratio between fluxes of heavier and lighter isotopologues ($F^{\text{heavy}}/F^{\text{light}}$):

$$F^{\text{heavy}}/F^{\text{light}} = \frac{-(K\overline{\rho_a}/M_a)\,\mathrm{d}\overline{[\text{heavy}]}/\mathrm{d}z}{-(K\overline{\rho_a}/M_a)\,\mathrm{d}\overline{[\text{light}]}/\mathrm{d}z} \tag{1}$$

where K is the eddy diffusivity, which was assumed to be the same for the heavy and light isotopologues, $\overline{\rho_a}$ is the mean density of dry air, M_a is the molar mass of dry air and $\mathrm{d}\overline{[\text{heavy}]}/\mathrm{d}z$ and $\mathrm{d}\overline{[\text{light}]}/\mathrm{d}z$ are the time-averaged vertical gradients of the heavy and light isotopologues measured simultaneously at the same height. For practical applications Eq. (1a) can be rewritten as

$$F^{\text{heavy}}/F^{\text{light}} = \frac{\overline{[\text{heavy}]}_{z_2} - \overline{[\text{heavy}]}_{z_1}}{\overline{[\text{light}]}_{z_2} - \overline{[\text{light}]}_{z_1}} \tag{2}$$

where $\overline{[\text{heavy}]}$ and $\overline{[\text{light}]}$ are the half-hour mean mixing ratios of isotopologues, measured at two heights (z_1 = 0.45 and z_2 = 1.45 m) near the forest floor. Large uncertainties in the estimates provided by the IFR method were observed when the gradient of $^{13}CO_2$ mixing ratio was smaller than 0.035 µmol mol^{-1} m^{-1}, which, considering the typical proportion of $^{13}CO_2$ in the air, corresponds to a gradient of CO_2 mixing ratio of approximately 3.2 µmol mol^{-1} m^{-1}. The same threshold was also observed by Griffis et al. (2005b). Hence, only half-hours, in which the difference of CO_2 mixing ratio between two measurement heights was larger than 5 µmol mol^{-1}, were used to calculate $F^{\text{heavy}}/F^{\text{light}}$, which was expressed in delta notation:

$$\delta_F = \frac{R_F}{R_{\text{VPDB}}} - 1 \tag{3}$$

where δ_F is the isotope ratio of the CO_2 flux, reported in parts per thousand (‰) in this study. R_F is the ratio between the heavier and lighter isotopologue fluxes (F^{heavy}/F^{light}) defined as F^{13}/F^{12} for $^{13}CO_2$ and $^{12}CO_2$ fluxes, or 0.5 F^{18}/F^{16} for $C^{18}O^{16}O$ and $C^{16}O_2$ fluxes, and R_{VPDB} is the molar ratio ($^{13}C/^{12}C$ or $^{18}O/^{16}O$) of Viena Peedee Belemnite.

The isotope composition of CO_2 flux ($\delta^{18}O_F$ and $\delta^{13}C_F$) provided by the IFR approach was compared to $\delta^{18}O_F$ and $\delta^{13}C_F$ estimates derived using a mKP technique. Pataki et al. (2003) recommended the use of a minimum CO_2 mixing ratio range of 75 µmol mol^{-1} to minimize the errors of the conventional KP approach used with ^{13}C flask sampling data spanning long periods (hours). However, one of the main limitations of applying KP technique to ^{18}O is the high variability of $\delta^{18}O$ of source water in leaves and soil at short time scales (i.e. hours) (Bowling et al., 2003a; Ogée et al., 2004; Griffis et al., 2005a). In this study we attempted to minimize this problem by applying the KP method to derive $\delta^{18}O_F$ for half-hourly periods using 5 min values of CO_2 mixing ratios, $\delta^{18}O_a$ and $\delta^{13}C_a$ measured at 1.45 m above the forest floor (mKP). During half-hour periods, the threshold of mixing ratio (75 µmol mol^{-1}) for conventional flask-based Keeling plot is unlikely to be met, so in this study the half-hour Keeling plot data were screened based on the range of mixing ratio (>25 µmol mol^{-1}) and R^2 values (>0.95). In addition, the type I regression was used to estimate the Keeling-plot intercept since some bias can be introduced with the type II (geometric) regression when the range of CO_2 mixing ratio is small (Zobitz et al., 2006). In this study we adopted the term mKP to designate the modified Keeling plot approach to emphasize that the period and range of CO_2 mixing ratio were different than what is usually used in the literature.

Estimates of $\delta^{18}O_F$ and $\delta^{13}C_F$ provided by the IFR method were also compared to the Lagrangian dispersion analysis proposed by Warland and Thurtell (2000) (hereafter, WT analysis). The WT analysis was used to infer half-hourly $^{12}C^{16}O_2$. $^{13}CO_2$ and $C^{18}OO$ fluxes near the forest floor. This formulation is based on Taylor's Lagrangian dispersion theory (Taylor, 1921) and assumes that the canopy is formed by several vertical source layers, each one with a specific value of source strength (S). Over time, each source layer releases a certain amount of matter or energy that is assumed to disperse in a Gaussian fashion. The vertical gradient of concentration (dC/dz) can then be obtained by adding the contributions from each source layer:

$$\left|\frac{dC}{dz}\right|_i = \sum_{j=1}^{m} \mathbf{M}_{ij} S_j \Delta z_j \tag{4}$$

where i and j are the concentration (C) and source (S) layer indices, respectively, m is the number of source layers, Δz_j is the thickness of the source layer j with respect to the vertical coordinate (z) and $\mathbf{M}$ is the dispersion matrix, calculated using profiles of vertical wind velocity (σ_w) and Lagrangian time scale (T_L). Equation (3) can be also used to solve the inverse problem (i.e. S from C). Further details on WT analysis calculations are shown in Appendix A.

The flux (F_j) for each source layer is given by

$$F_j = \sum_{j=1}^{m} S_j \Delta z_j \tag{5}$$

Estimated $^{12}C^{16}O_2$, $^{13}CO_2$ and $C^{18}OO$ fluxes for the ground level source layer (S_1) were converted to delta notation using Eq. (3) and compared with the IFR estimates. To do that, Δz_1 was set to 1.4 m to match the two lowest concentration intake heights.

2.5 Modeling $\delta^{18}O_F$

The $\delta^{18}O$ of CO_2 flux obtained near the forest floor using the IFR approach was compared with estimates of $\delta^{18}O$ of net soil CO_2 flux ($\delta^{18}O_R$) obtained using an analytical model (Tans, 1998; Wingate et al., 2009). This formulation assumes isothermal and uniform soil water conditions to estimate $\delta^{18}O_R$:

$$\delta^{18}O_R = \delta^{18}O_{eq,s} + \varepsilon_{d,eff} + \left(\delta^{18}O_{eq,s} - \delta^{18}O_a\right) v_{inv} \frac{C_a}{F_R} \tag{6}$$

where $\delta^{18}O_{eq,s}$ (‰, VPDB) is the $\delta^{18}O$ of CO_2 in isotopic equilibrium with the soil water, $\varepsilon_{d,eff}$ is the effective isotopic fractionation during CO_2 diffusion in soil pores, C_a is the CO_2 molar concentration (µmol m^{-3}) obtained at 0.45 m above the forest floor and F_R is the soil CO_2 flux (µmol m^{-2} s^{-1}) measured using soil chambers (Sect. 2.3), v_{inv} (m s^{-1}) represents the rate at which CO_2 in a column of air exchanges its oxygen atoms with liquid water in the soil (Tans, 1998), which is given by

$$v_{inv} = \sqrt{B\theta_w k_s D_{18}} \tag{7}$$

where B is the Bunsen solubility coefficient for CO_2 (Weiss, 1974, $B = 1.739 \times \exp(-0.0390 \times T_s + 0.000236 \times T_s^2)$, θ_w is the soil water content (m^3 m^{-3}), D_{18} is the effective diffusivity of $C^{18}OO$ in soil air, k_s is effective rate of oxygen isotope exchange between CO_2 and liquid water (s^{-1}):

$$k_s = f_{CA} k_h \tag{8}$$

where f_{CA} is the relative increase in hydration resulting from the CA in the soil (Riley et al., 2003; Seibt et al., 2006; Wingate et al., 2008) and k_h is the rate of oxygen isotope exchange between CO_2 and water, equal to $1/3 \times 0.037 \times \exp^{[0.118 \times (Ts-25)]}$ (Skirrow, 1975; Wingate et al., 2008). Additional details on calculations of parameters used to model $\delta^{18}O_R$ are shown in Appendix B.

3 Results and discussion

3.1 Environmental conditions and temporal dynamics of CO_2 isotopes in the air near the forest floor

Rainfall was well-distributed throughout the experiment with the largest daily totals occurring at the end of July (DOY = 207) and beginning of August (DOY 221) (Fig. 4a). The total precipitation from July to September was 190 mm, which was above the long-term average (144 mm) from 1989 to 2006 for a nearby weather station (Egbert, Environment Canada, 2009). The daily average air temperature during the experiment was slightly cooler (17.5 °C) than the long-term average (17.8 °C). Air temperature reached its maximum in August (DOY 229) and then presented a downward trend until the end of the period (Fig. 4a). Average soil temperature at 10 cm was equal to 22 °C over the study period. Large precipitation events and good drainage favoured by sandy soil at the site (Table 1) contributed to the occurrence of significant variability in the soil water content throughout the season, with soil water content ranging from 0.08 to 0.18 $m^3\,m^{-3}$ at 10 cm depth (Fig. 4b). The half-hourly soil CO_2 flux (F_R) showed similar temporal variation as the soil water content. Higher values of F_R($\sim$6.5 $\mu mol\,m^{-2}\,s^{-1}$, DOY 205) were observed when soil water content values were high, while smaller magnitudes of soil respiration (3.1 $\mu mol\,m^{-2}\,s^{-1}$, DOY 220) were observed during dry periods (Fig. 4c). The ensemble-averaged CO_2 mixing ratio (86 days), $\delta^{18}O_a$ and $\delta^{13}C_a$ obtained near the forest floor show a distinct diurnal pattern (Fig. 5). The CO_2 mixing ratio reached its minimum (379 $\mu mol\,mol^{-1}$) in the early afternoon (13:30 h EST), and its maximum (465 $\mu mol\,mol^{-1}$) at 08:30 h EST. Data points during liquid nitrogen refilling time were excluded from this Fig. Conversely, $\delta^{18}O_a$ became less negative reaching its maximum value (−0.39 ‰) in the early afternoon and minimum (−2.63 ‰) in the morning. Values of $\delta^{13}C_a$ showed a similar daily trend as $\delta^{18}O_a$, with values ranging from −11.01 to −7.94 ‰. The causes of this daily pattern of $\delta^{18}O_a$ and $\delta^{13}C_a$, the expansion of daytime boundary layer, the entrainment of air enriched in ^{13}C, and ^{18}O during the daytime and the buildup of CO_2 depleted in the heavy isotopes originated from the soil during low turbulence conditions in the nighttime (Griffis et al., 2004, 2005a; Seibt et al., 2006).

3.2 Comparison between isotope flux ratio and Keeling plot approaches

The comparison between $\delta^{18}O_F$ and $\delta^{13}C_F$ estimated using the mKP and IFR methods is shown in Fig. 6. The averages of mKP standard error of intercept were equal to 0.9 ‰ and 1.3 ‰ for $\delta^{18}O_F$ and $\delta^{13}C_F$, respectively. Only 17 % ($\delta^{18}O_F$) and 24 % ($\delta^{13}C_F$) of the half-hours analyzed met the criteria used to screen the mKP estimates (CO_2 range >25 $\mu mol\,mol^{-1}$ and $R^2 > 0.95$). The intercept error was much larger (3.4 and 3.7 ‰, for $\delta^{18}O_F$ and $\delta^{13}C_F$, respectively) when R^2 was not used to screen mKP data. Conversely, 95 % of the half-hour intervals met the criterion used to screen the IFR data obtained close to the forest floor, i.e. difference of CO_2 mixing ratio between the two air intakes near the forest floor was larger than 5 $\mu mol\,mol^{-1}$. The estimates of $\delta^{18}O_F$ provided by the IFR method showed good correlation (R^2 = 0.80) and agreement (slope = 1.03) with estimates of $\delta^{18}O_F$ obtained using the mKP technique. The regression analysis coefficients were not significant for $\delta^{13}C_F$ ($P < 0.01$). This can be explained by the relatively large uncertainties in mKP and IFR estimates in comparison to the small range of $\delta^{13}C_F$ values observed for this ecosystem. The mean (±SE) mKP and IFR $\delta^{13}C_F$ values were −27.5 ‰ (±0.2) and −27.3 ‰ (±0.1), respectively, both within the range of values reported for soil respiration of C_3 ecosystems (Buchmann et al., 1997; Bowling et al., 2005), which provides evidence supporting the validity of these methods inside the forest. Student's t-test showed that the two estimates for $\delta^{13}C_F$ were not different statistically ($P > 0.05$).

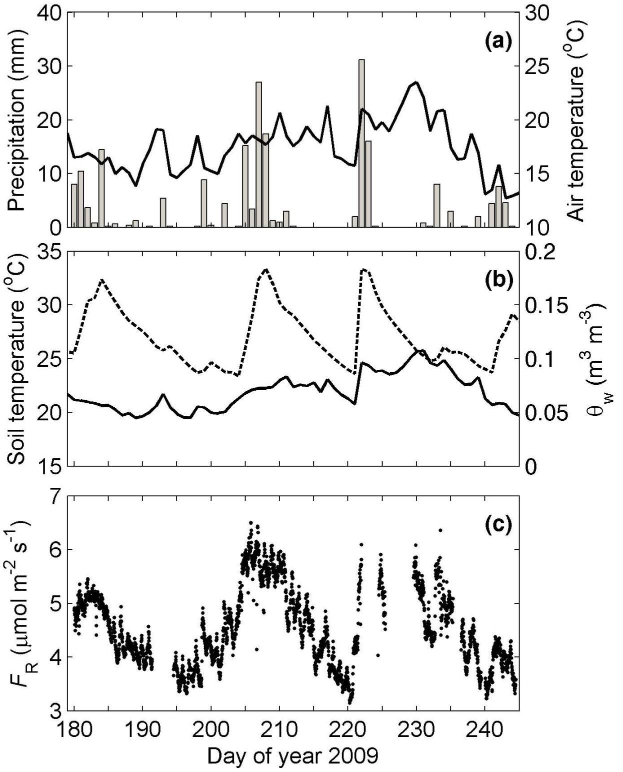

Fig. 4. (a) Daily total precipitation (bars) and mean air temperature (solid line), **(b)** daily mean soil temperature (solid line) and mean soil volumetric water content (θ_W, dashed line) at 10 cm depth, **(c)** half-hourly soil CO_2 flux (F_R). The gaps observed in F_R data were caused by automatic soil chamber failure.

The KP approach has been widely used to determine the $^{13}CO_2$ composition of ecosystem respiration (Pataki et al., 2003). However, previous studies have shown that this approach may not be reliable for inferring the $\delta^{18}O$ of CO_2

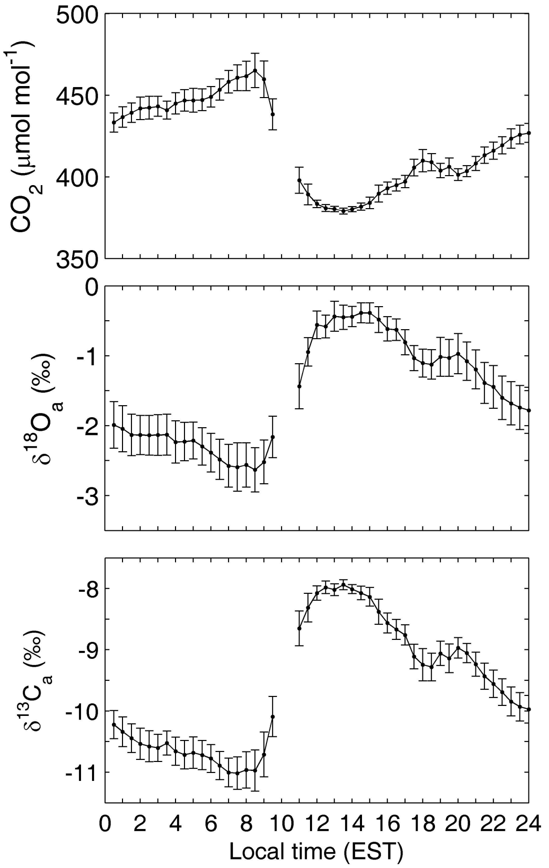

Fig. 5. Ensemble half-hourly average of CO_2 mixing ratio and isotopic compositions of CO_2 ($\delta^{18}O_a$ and $\delta^{13}C_a$, VPDB scale) in the air at 1.45 m above the floor of a deciduous temperate forest from day of the year 188 to 274 in 2009. The error bars indicate ±1 mean standard error. Data from 10:00 to 11:00 h (EST) were discarded due to liquid nitrogen filling time, which resulted in fewer data points than the remaining hours of the day.

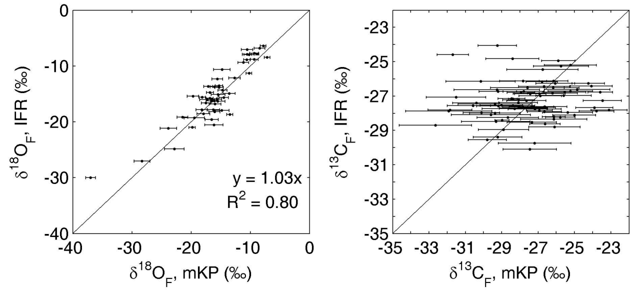

Fig. 6. Relationship between half-hourly isotopic ratios of the CO_2 flux near the forest floor ($\delta^{18}O_F$, $\delta^{13}C_F$) estimated using Keeling plot (± standard error of intercept) and isotopologue ratio method in the understory of a deciduous forest.

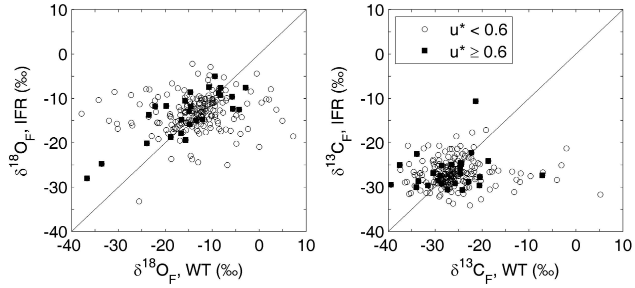

Fig. 7. Relationship between half-hourly isotopic ratios of the CO_2 flux near the forest floor ($\delta^{18}O_F$ and $\delta^{13}C_F$) estimated using a Lagrangian dispersion analysis (WT analysis) and flux ratio method in the understory of a deciduous forest. u_* is the friction velocity ($m\,s^{-1}$).

flux (Flanagan et al., 1997; Ogée et al., 2004; Griffis et al., 2005a). Tans (1998) demonstrated that the use of KP approach to estimate $\delta^{18}O_R$ could lead to significant error due the ^{18}O exchange between CO_2 in the air and soil water, which is also known as abiotic flux or non-respiratory invasion flux (F_{inv}) (Miller et al., 1999; Riley, 2005), defined as the product of v_{inv} (Eq. 6) and C_a. Tans (1998) showed that the magnitude of the error in the derived $\delta^{18}O_R$ using the KP approach is proportional to F_{inv}/F_R. His simulations indicate that an error of 3 ‰ could occur in $\delta^{18}O_F$, derived using the KP approach, when F_{inv}/F_R is 0.5 and an error of 9 ‰ would be expected for $F_{inv}/F_R = 2$. In this study the ratio between modeled F_{inv} and measuredF_R was calculated for half-hour periods (shown in Fig. 6), in which $\delta^{18}O_F$ was compared with the mKP approach. The average F_{inv}/F_R for these periods was 0.13, and the maximum value for this ratio was 0.19, considering $f_{CA} = 1$. The good agreement between the IFR and mKP $\delta^{18}O_F$ estimates is encouraging, but we acknowledge that the magnitude of F_{inv} could be larger due to the activity of the enzyme carbonic anhydrase in the soil (Eqs. 7 and 8). The effect of this enzyme on the CO_2 hydration in the soil is not fully understood and shows large temporal and spatial variation (Seibt et al., 2006; Wingate et al., 2008, 2010).

3.3 Isotope flux ratio and WT analysis comparisons

Estimates of $\delta^{18}O_F$ and $\delta^{13}C_F$ obtained using the IFR were compared with $\delta^{18}O_F$ and $\delta^{13}C_F$ obtained using the WT analysis (Fig. 7). This comparison was only performed for a 23-day period (DOY 237 to 260), when the eight air intakes were sampled continuously within and above the forest canopy. The regression analysis coefficients were not significant ($P > 0.05$) for the relationships between $\delta^{18}O_F$ and $\delta^{13}C_F$ obtained using IFR and mKP methods. Santos et al. (2011) observed that the WT analysis yielded spurious estimates of CO_2 flux for the lowest source layer in a corn canopy. They hypothesize that the poor performance of the WT analysis was observed when the flows above and within the canopy were decoupled due to poor mixing within the corn canopy. In this study the regression analysis coefficients for the relationship between WT analysis and

IFR $\delta^{18}O_F$ were significant ($y = -9.9 + 0.28x$, $R^2 = 0.37$, $P < 0.01$) when only half-hour periods with friction velocity (u_*) $\geq 0.6\,\mathrm{m\,s^{-1}}$ were included. The mean difference between $\delta^{13}C_F$ estimated by mKP and IFR methods was not statistically significant based on Student's t-test ($P > 0.05$), as observed previously for the comparisons between mKP and IFR methods. The WT analysis could be used to study isotope exchange within plant canopies; however, additional evaluation of this methodology under different turbulence conditions is still required and needs to be performed in future studies.

A concern that is generally raised when using gradient-diffusion based methods is the occurrence of counter-gradient fluxes within canopies. Corrsin (1974) observed that a description of the turbulent exchange of scalars using the gradient-diffusion theory is only feasible if the length scale of turbulence is much smaller than the distance over which the gradient of concentration of the transported scalar changes. Wilson (1989) demonstrated that near elevated sources, such as plant canopies, there are substantial changes in gradients of concentration of transported entities over distances much smaller than the length scale of turbulence, expressed by $\sigma_w T_L$, leading to counter-gradient fluxes in some situations. Raupach (1987) used a Lagrangian homogeneous turbulence formulation to demonstrate how counter-gradient fluxes arise in plant canopies. His results showed that counter-gradient fluxes are expected to occur when the transported entity source profile strength shows an intense and localized peak in the foliage well above the ground; however, his simulations do not indicate the occurrence of counter-gradient fluxes in the trunk space near the ground. Wilson (1989) observed that the magnitudes of σ_w and T_L are small in relation to the gradient of concentration near the surface (Fig. A1), so the gradient-diffusion theory is suitable to investigate the transport of scalars near ground-level sources. Furthermore, previous studies have confirmed the suitability of gradient-diffusion based methods to study scalar exchange in the open trunk space of forests (Dolman and Wallace, 1991; Baldocchi and Meyers, 1991; Wu et al., 2001). These studies and the results obtained here indicate that the IFR is suitable to investigate the isotope exchange in the trunk space near the forest floor.

3.4 Comparison between isotope flux ratio estimates and modeled $\delta^{18}O_R$

The $\delta^{18}O_F$ estimated by the IFR approach near the forest floor was compared with modeled $\delta^{18}O_R$ (Eq. 5) to investigate the impact of environmental variables on the temporal dynamics of $\delta^{18}O_F$ during four selected periods (Fig. 8). These periods were selected because all the measurements required for modeling $\delta^{18}O_R$ were available and the sampling system was being used exclusively to measure the air intakes near the forest floor, resulting in a larger number of data points for each intake and consequently improving the ability of the TGA to measure concentration differences between air intakes (Wagner-Riddle et al., 2005).

Values of F_R during the four selected periods ranged from 3.2 (DOY 220) to 6.4 $\mu\mathrm{mol\,mol^{-1}}$ (DOY 206) and showed good correlation with the soil temperature (data not shown). Soil water content showed large variation between selected periods as a result of precipitation events and the good soil drainage at the site. During a dry period (DOY 199 to 201), values of θ_w showed small variations and average of 10 %; on the other hand for a rainy period (DOY 206 to 208), θ_w was higher reaching 23 % after a precipitation event (DOY 206). Average $\delta^{18}O_a$ was −2.9 ‰; however, more depleted $\delta^{18}O_a$ values (−6.3 ‰) were observed after a precipitation event on DOY 207. $\delta^{18}O_{sw}$ sampled at 10 cm did not show large variations between sampling dates, and further considerations on the $\delta^{18}O_{sw}$ impact on model calculations will be discussed below.

Figure 8 show also comparisons between $\delta^{18}O_F$ and modeled $\delta^{18}O_R$. These comparisons rely on the assumption that the variation in $\delta^{18}O_F$ is mainly caused by $\delta^{18}O_R$ dynamics. This was considered a valid assumption since flux ratio measurements were obtained near the ground and the vegetation in the forest understorey was sparse. Estimated values of $\delta^{18}O_F$ using the IFR method ranged from −31.4 ‰ (DOY 208) to −11.2 ‰ (DOY 221). Large variations in $\delta^{18}O_F$ were observed on DOY 206 to 208, when precipitation events caused a reduction in $\delta^{18}O_F$ of approximately 8 ‰ from nighttime periods of DOY 207 to 208. A diurnal variation in $\delta^{18}O_F$ was observed on DOY 213, 220 and 221, with more depleted $\delta^{18}O_F$ present during daytime.

Wingate et al. (2010) also reported more depleted $\delta^{18}O_R$ values in the daytime in a maritime pine stand, which were synchronized with variations in $\delta^{18}O_a$ and F_R. In their study $\delta^{18}O_a$ was more enriched during the daytime, similarly to the $\delta^{18}O_a$ daily trend observed in the present study (Fig. 5). On the other hand, Seibt et al. (2006) observed an opposite trend in $\delta^{18}O_a$ close to the soil surface, with values around 3 ‰ during the night- and −2 ‰ in the daytime. They observed that daily variations in $\delta^{18}O_R$ were coupled with $\delta^{18}O_a$. In this study $\delta^{18}O_a$ and $\delta^{18}O_R$ were not well coupled (Fig. 8) and this could not explain diel changes in $\delta^{18}O_R$. One hypothesis to explain our daily variations in $\delta^{18}O_R$ is that diel variations in $\delta^{18}O_{sw}$ could lead to changes in $\delta^{18}O_R$, but a more frequent soil water sampling scheme would be required to test this hypothesis.

The mean differences between $\delta^{18}O_F$ and modeled $\delta^{18}O_R$ over the whole period were equal to 4.2, 0.53 and 4.8 ‰ for f_{CA} = 1, 20 and 100, respectively (Fig. 8). Wingate et al. (2010) observed that a temporally uniform f_{CA} = 70 improved the agreement between modeled $\delta^{18}O_{sw}$ and estimated from the oxygen composition of the net CO_2 flux obtained during a 20-day period. Our results show that the use of f_{CA} = 20 could minimize the differences between $\delta^{18}O_F$ and modeled $\delta^{18}O_R$ over the whole period. However, the use of a single value of f_{CA} over the whole period could

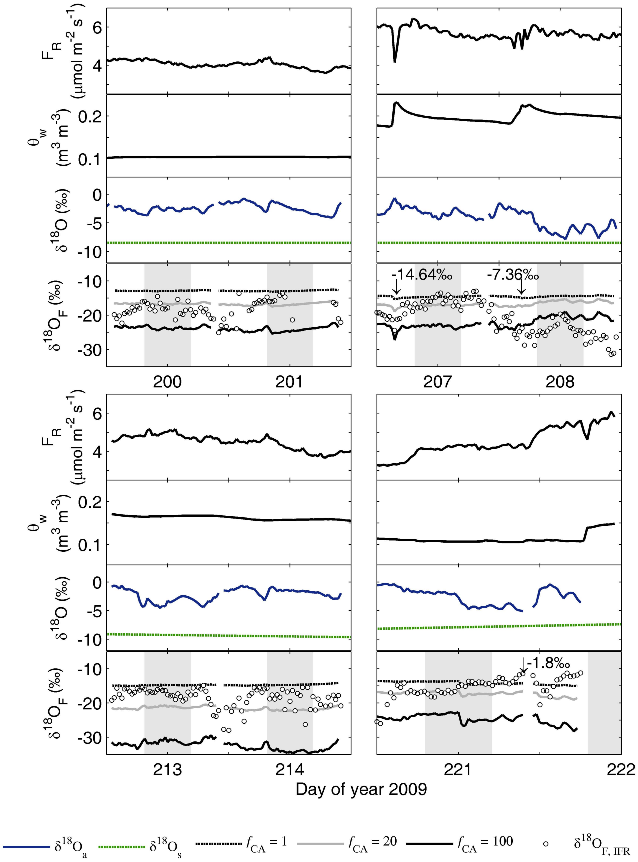

Fig. 8. Half-hour values of soil CO_2 flux (F_R), soil water content (θ_w) and $C^{18}OO$ composition of the air (δ^{18}Oa, blue solid line), expressed using the VPDB scale, during four selected periods. $H_2^{18}O$ composition of the soil water (δ^{18}Os, VSMOW scale) at the 10 cm depth between two sampling dates. $C^{18}OO$ composition of CO_2 flux ($\delta^{18}O_F$) near the forest floor obtained using the isotope flux ratio method ($\delta^{18}O_{F,IFR}$, open circles) and modeled δ^{18}O of net soil CO_2 flux (lines) according to Wingate et al. (2009) using three values for the relative increase in hydration due to the enzyme carbonic anhydrase activity in the soil (f_{CA}, Eq. 7) in a temperate deciduous forest. The δ^{18}O of CO_2 flux is expressed in the VPDB scale. Shaded areas in the graph indicate nighttime periods, and arrows indicate precipitation events with respective isotope composition of precipitation water expressed in the VSMOW scale.

not explain diel variations in $\delta^{18}O_F$. The daytime depletion in $\delta^{18}O_F$ (DOY 200, 213 and 220), for example, required larger values of f_{CA} to improve the daytime agreement between modeled and measured values when compared to the f_{CA} values used for the nighttime. Seibt et al. (2006) used a multi-layer model to study the temporal dynamics of $\delta^{18}O_R$ in a *P. sitchensis* plantation. Their results also indicate large temporal variation of f_{CA}, requiring the use of f_{CA} values ranging from 80 to 1000 for soil top layer to match chamber observations during three sampling campaigns. The use of large values of f_{CA} results in shallower z_{eq} (see Appendix B). In this study typical values of z_{eq} were 7, 1.5 and 0.6 cm for f_{CA} = 1, 20 and 100, respectively. We acknowledge that the extrapolation of $\delta^{18}O_{sw}$ beyond the sampling depths could lead to errors in $\delta^{18}O_R$ estimates, especially when large gradients of $\delta^{18}O_{sw}$ were observed close to the soil surface (DOY 211, Fig. 3). An arbitrary reduction of 2 ‰ (VSMOW) in $\delta^{18}O_{sw}$ resulted in a decrease of ~4 ‰ (VPDB) in $\delta^{18}O_R$ values, assuming f_{CA} = 100. Thus, more superficial soil sampling could be beneficial when using this model for estimating $\delta^{18}O_R$.

On DOY 220 to 222 $\delta^{18}O_F$, values showed an upward trend, which was coupled with F_R variation; however, this trend was not captured by the $\delta^{18}O_R$ model. Wingate et al. (2008) observed that, besides the effect of the CA, an evaporative enrichment of 3 ‰ in $\delta^{18}O_{sw}$ values was required to improve the agreement between modeled $\delta^{18}O_R$ and soil chamber observations during a 3-day period in a Mediterranean soil. In this study, an enrichment of ~2.5 ‰ (VSMOW) in $\delta^{18}O_{sw}$ from DOY 220 to 222 (before precipitation event) would be necessary to improve the agreement between modeled $\delta^{18}O_R$ and measured $\delta^{18}O_F$ for a constant f_{CA} = 20.

Large disagreement between modeled $\delta^{18}O_R$ and $\delta^{18}O_F$ was observed after precipitation events, which was likely due to changes in $\delta^{18}O_{sw}$. A decrease of approximately 5 ‰ in $\delta^{18}O_{sw}$ would be required to match measured with modeled $\delta^{18}O_R$ values on the nighttime of DOY 208, assuming a constant f_{CA} = 20. These results show that changes in $\delta^{18}O_{sw}$ caused by precipitation events are unlikely to be properly represented by the weekly soil water sampling scheme performed in this study. The proper characterization of $\delta^{18}O_{sw}$ would require more frequent soil sampling or $\delta^{18}O_{sw}$ modeling approaches that take the δ^{18}O of precipitation into consideration (Braud et al., 2005; Wingate et al., 2010).

4 Conclusions

The IFR and mKP methods showed very good agreement (slope = 1.03) and good correlation (R^2 = 0.80) when used to estimate half-hourly $\delta^{18}O_F$. The mean (±SE) mKP and IFR $\delta^{13}C_F$ values were −27.5 ‰ (±0.2) and –27.3 ‰ (±0.1), respectively, both within the range of values reported for soil respiration of C_3 ecosystems (Bowling et al., 2005), which provides evidence supporting the validity of these methods inside the forest. The comparisons between IFR and mKP techniques are encouraging, as they show that the IFR method can be used to study the isotope exchange near the forest floor. The large amount of data captured (~95 % of half-hour periods evaluated) for the IFR method compared to the mKP method provides new opportunities for the study of $\delta^{18}O_F$ dynamics within forest canopies.

The coefficients of the regression analysis between WT analysis and IFR were not significant ($P > 0.05$). However, better correlation ($R^2 = 0.37$) between WT analysis and IFR $\delta^{18}O_F$ was obtained when only turbulent periods ($u_* \geq 0.6\,\mathrm{m\,s^{-1}}$) were included in the analysis. During low turbulence periods, the decoupling between above and within canopy flows could be one of the reasons for the poor agreement between the two methods. Further investigation on the use of the WT analysis to study the isotope exchange in ecosystems is still necessary.

The δ^{18}O of CO$_2$ flux near the forest floor showed large temporal variation, with values ranging from –31.4 ‰ (DOY 208) to –11.2 ‰ (DOY 221). Precipitation events caused substantial variation (∼8 ‰) in $\delta^{18}\mathrm{O_F}$ over a period of approximately 24 h. A diel trend of $\delta^{18}\mathrm{O_F}$ was also observed, with more negative values being observed during the daytime. The use of a single value of f_CA over the whole period could not explain the diel variation of $\delta^{18}\mathrm{O_F}$. The results also show the importance of a frequent soil sampling scheme for the accuracy of modeled $\delta^{18}\mathrm{O_R}$ values.

Appendix A

WT analysis and turbulence statistics calculations

Warland and Thurtell (2000) used a dispersion matrix (**M**) to relate the concentration profile with the source strength distribution of transported scalars within plant canopies (Eq. 4). A full description of this analysis and details in the derivation of **M** can be found in Warland and Thurtell (2000). The dispersion matrix **M** is calculated using turbulence statistics at source and concentration measurement heights:

$$\mathbf{M}_{ij} = \begin{cases} \dfrac{-\left[1-\exp\left(\frac{-(z_i-z_j)^2}{2\Delta z_j^2}\right)\right]}{2\sigma_{\mathrm{w}i} L_{\mathrm{L}i}\left[1-\exp\left(-\sqrt{\frac{\pi}{2}}\frac{(z_i-z_j)}{(L_{\mathrm{L}i}+L_{\mathrm{L}j})/2}\right)\right]} + G_{ij} & \text{for } z_i > z_j \\ G_{ij} & \text{for } z_i = z_j \\ \dfrac{\left[1-\exp\left(\frac{-(z_i-z_j)^2}{2\Delta z_j^2}\right)\right]}{2\sigma_{\mathrm{w}i} L_{\mathrm{L}i}\left[1-\exp\left(-\sqrt{\frac{\pi}{2}}\frac{(z_j-z_i)}{(L_{\mathrm{L}i}+L_{\mathrm{L}j})/2}\right)\right]} + G_{ij} & \text{for } z_i < z_j \end{cases} \tag{A1}$$

where L_L is the Lagrangian length scale, given by $L_L = \sigma_w T_L$, z_i and z_j are the heights of the concentration measurements i and of the source layer j, respectively, and $\boldsymbol{G}_{ij}$ represents the image source, specified to create a reflecting boundary (Warland and Thurtell, 2000):

$$\boldsymbol{G}_{ij} = \frac{-\left[1-\exp\left(\frac{-(z_i+z_j)^2}{2\Delta z_j^2}\right)\right]}{2\sigma_{\mathrm{w}i} L_{\mathrm{L}i}\left[1-\exp\left(-\sqrt{\frac{\pi}{2}}\frac{(z_i+z_j)}{(L_{\mathrm{L}i}+L_{\mathrm{L}j})/2}\right)\right]} \tag{A2}$$

The parameterizations of turbulence statistics proposed by Leuning et al. (2000) and Styles et al. (2002) were used to estimate σ_w and T_L profiles, respectively (Fig. A1). Leuning et al. (2000) used exponential and non-rectangular hyperbolic functions to describe the profile of σ_w:

$$\frac{\sigma_\mathrm{w}}{u_*} = c_1 e^{c_2 z/h} \quad \text{for } z < 0.8\,h \tag{A3a}$$

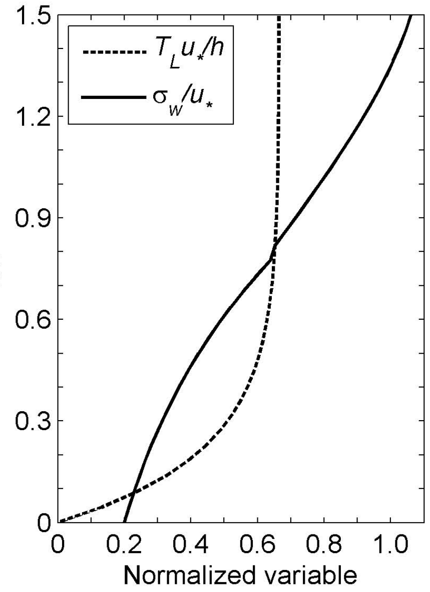

Fig. A1. Normalized profiles of Lagrangian time scale (T_L) and standard deviation of vertical wind velocity (σ_w), calculated using the parameterizations proposed by Styles et al. (2002) and Leuning (2000), respectively.

$$\frac{\sigma_\mathrm{w}}{u_*} = \frac{(az/h+b)+d_1\sqrt{(az/h+b)^2-4\theta abz/h}}{2\theta} \quad \text{for } z \geq 0.8\,h \tag{A3b}$$

where u_* is the friction velocity, obtained using sonic anemometer set up at 33.4 m (Sect. 2.3), h is the canopy height, $c_1 = 0.2$, $c_2 = 1.5$, $a = 0.85$, $b = 0.4$, $d_1 = -1$ and $\theta = 0.98$. The σ_w profiles obtained using these equations are in agreement with turbulence measurements, reported by Raupach (1989b) and obtained for seven different canopies (two corn and forest canopies and three wind tunnel models).

Styles et al. (2002) proposed the following function to describe the profile of T_L within and just above plant canopies:

$$T_\mathrm{L} = c_4 \frac{1-\exp(-c_3 \cdot z/h)}{1-\exp(-c_3)} \frac{h}{u_*} \tag{A4}$$

where c_3 and c_4 are fitted coefficients. We adopted values for c_3 (= 4.86) and c_4 (= 0.10), obtained by Haverd et al. (2009), using an optimization procedure to improve the agreement between modeled and measured concentration profiles of temperature, water vapour and CO$_2$ concentration in a temperate eucalyptus forest. The parameterizations of turbulence statistics described above were developed under neutral atmospheric conditions, so atmospheric stability functions proposed by Leuning (2000) were used to correct the profiles of σ_w and T_L for non-neutral conditions.

Equation (4) needs to be integrated to be used with discrete measurements. This integration was performed using the trapezoidal rule from the concentration measurement height (z_i) to the reference height ($z_\mathrm{R} = 36.81$ m), reducing the sensitivity of the source to small gradients between adjacent heights when solving the inverse problem (Qiu and

Warland, 2006):

$$C_r - C_i = \sum_{i=1}^{n-1}\sum_{j=1}^{m}\frac{1}{2}\left(\mathbf{M}_{ij}+\mathbf{M}_{(i+1)j}\right)S_j\,\Delta z_j\,\Delta z_i \tag{A5}$$

where C_r and C_i are the concentrations at z_R and z_i, respectively, m (= 4) is the number of source layers, and n (= 8) is and the number of concentration measurement heights. The use of redundant concentration data ($n > m$) reduces source strength uncertainties originating from errors in the concentration or turbulence statistics profiles (Raupach, 1989b). In the present study, a layer thickness $\Delta z_i = 0.01\,\mathrm{m}$ was used in Eq. (A5), following Qiu and Warland (2006). $C^{16}O_2$ and $C^{18}OO$ source strengths were inferred within the forest canopy using concentration measurements obtained when the TGA sampling system was set to sample eight air intakes within and above the forest canopy (Sect. 2.2).

Appendix B

Calculation of parameters used to model δ^{18}O of soil CO_2 flux

The isotope composition of CO_2 in isotopic equilibrium with the soil water (Brenninkmeijer et al., 1983), used in Eq. (6), was calculated as follows:

$$\delta^{18}\mathrm{O}_{\mathrm{eq,s}} = \delta^{18}\mathrm{O}_{\mathrm{sw}} + \frac{17604}{(T_\mathrm{s}+273.16)} - 17.93 \tag{B1}$$

where $\delta^{18}\mathrm{O}_{\mathrm{sw}}$ is the isotopic composition of soil water at the equilibration depth (z_{eq}), $z_{\mathrm{eq}} = 2\sqrt{2\ln 2 D_{18}/k_s B\theta_w}$, which is defined as the shallowest depth at which full isotopic equilibration between water and CO_2 molecules occurs (Wingate et al., 2009). $\delta^{18}\mathrm{O}_{\mathrm{sw}}$ profiles were obtained as described in Sect. 2.3 and were converted into the VPDB scale to be used in Eq. (B1). The effective kinetic fractionation ($\varepsilon_{\mathrm{d,eff}}$) was calculated following Wingate et al. (2009):

$$\varepsilon_{\mathrm{d,eff}} = \varepsilon_{\mathrm{d}}\left\{1 - \frac{z_1}{z_0}\left[1-\exp\left(-z_0/z_1\right)\right]\right\} \tag{B2}$$

where ε_d is the full kinetic fractionation during CO_2 diffusion in soil pores, equal to –8.7 ‰ (Tans, 1998), $z_1 = z_{\mathrm{eq}}\left(2\sqrt{2\ln 2}\right)^{-1}$, and z_o is the soil column depth over which uniform CO_2 production occurs, assumed to be equal to 0.15 m in this study (Riley et al., 2003).

The effective diffusivity of $C^{18}OO$ in soil air is given by $D_{18} = D_\mathrm{s}\alpha_d$, with $\alpha_d = 1 + \varepsilon_d/1000$, and D_s the diffusivity of CO_2 in soil air (Moldrup et al., 2003):

$$D_\mathrm{s} = D_{25}\theta_\mathrm{a}^2\left(\frac{\theta_\mathrm{a}}{\theta_{\mathrm{sat}}}\right)^{\frac{3}{b}}\left(\frac{T_\mathrm{s}+273.16}{T_{25}}\right)^n \tag{B3}$$

where D_{25} is the molecular diffusivity of CO_2 ($1.4\times10^{-5}\,\mathrm{m^2\,s^{-1}}$) at 298 K; θ_a is the proportion of soil pores filled with air; $\theta_\mathrm{a} = \theta_{\mathrm{sat}} - \theta_\mathrm{w}$, where θ_{sat} is the soil water content at saturation estimated to be $0.46\,\mathrm{m^3\,m^{-3}}$ at the site (Saxton and Willey, 2006), b is the soil water retention parameter, determined to be equal to 6.2 in this study (Cosby et al., 1984), $T_{25} = 298\,\mathrm{K}$ and n is 1.5 (Bird et al., 2002).

Acknowledgements. Funding for this research was provided by the Natural Science and Engineering Research Council. The first author was funded by Brazilian National Council for Scientific and Technological Development (CNPq). Xuhui Lee acknowledges support by the US National Science Foundation through grant ATM-0914473. We would also like to thank the two anonymous reviewers for their helpful suggestions.

Edited by: U. Seibt

References

Allison, C. A., Francey, R. J., and Meijer, H. A. J.: Recommendations for the reporting of stable isotope measurements of carbon and axygen in CO_2 gas, Reference and intercomparison materials for stable isotopes of light elements, IAEA-TECDOC, 825, 155–162, 1995.

Amundson, R., Stern, L., Baisden, T., and Wang, Y.: The isotopic composition of soil and soil-respired CO_2, Geoderma, 82, 83–114, 1998.

Baldocchi, D. D. and Meyers, T. P.: Trace gas-exchange above the floor of a deciduous forest 1. Evaporation and CO_2 efflux, J. Geophys. Res.-Atmos, 96, 7271–7285, 1991.

Bird, R. B., Stewart, W. E., and Ligthfoot, E. N. Transport phenomena. Wiley, New York, 2002.

Bowling, D. R., Tans, P. P., and Monson, R. K.: Partitioning net ecosystem carbon exchange with isotopic fluxes of CO_2, Glob. Change Biol., 7, 127–145, 2001.

Bowling, D. R., Mcdowell, N. G., Welker, J. M., Bond, B. J., Law, B. E., and Ehleringer, J. R.: Oxygen isotope content of CO_2 in nocturnal ecosystem respiration: 2. Short-term dynamics of foliar and soil component fluxes in an old-growth ponderosa pine forest, Global Biogeochem. Cy., 17, 1124, doi:10.1029/2003GB002082, 2003a.

Bowling, D. R., Sargent, S. D., Tanner, B. D., and Ehleringer, J. R.: Tunable diode laser absorption spectroscopy for stable isotope studies of ecosystem-atmosphere CO_2 exchange, Agr. Forest Meteorol., 118, 1–19, 2003b.

Bowling, D. R., Burns, S. P., Conway, T. J., Monson, R .K., and White, J. W. C.: Extensive observations of CO_2 carbon isotope content in and above a high-elevation subalpine forest, Global Biogeochem. Cy., 19, GB3023, doi:10.1029/2004GB002394, 2005.

Braud, I., Bariac, T., Gaudet, J. P., and Vauclin, M.: Sispat-isotope, a coupled heat, water and stable isotope (HDO and $H_2^{18}O$) transport model for bare soil. Part I. Model description and first verifications, J. Hydrol., 309, 277–300, 2005.

Brenninkmeijer, C. A. M., Kraft, P., and Mook, W. G.: Oxygen isotope fractionation between CO_2 and H_2O, Isot. Geosci., 1, 181–190, 1983.

Buchmann, N., Kao, W. Y., and Ehleringer, J.: Influence of stand structure on carbon-13 of vegetation, soils, and canopy air within deciduous and evergreen forests in Utah, United States, Oecologia, 110, 109–119, 1997.

Ciais, P., Tans, P. P., White, J. W. C., Trolier, M., Francey, R. J., Berry, J. A., Randall, D. R., Sellers, P. J., Collatz, J. G., and Schimel, D. S.: Partitioning of ocean and land uptake of CO_2 as inferred by δ^{13}C measurements from the NOAA climate monitoring and diagnostics laboratory global air sampling network., J. Geophys. Res.-Atmos, 100, 5051–5070, 1995.

Corrsin, S.: Limitations of gradient transport models in random walks and in turbulence, Adv. Geophys., 18A, 25–60, 1974.

Cosby, B. J., Hornberger, G. M., Clapp, R. B., and Ginn, T. R.: A statistical exploration of the relationships of soil-moisture characteristics to the physical-properties of soils, Water Resour. Res., 20, 682–690, 1984.

Cuntz, M., Ciais, P., Hoffmann, G., and Knorr, W.: A comprehensive global three-dimensional model of δ^{18}O in atmospheric CO_2: 1. Validation of surface processes, J. Geophys. Res.-Atmos, 108, 4527, doi:10.1029/2002JD003153, 2003.

Davidson, E. A., Savage, K., Verchot, L. V., and Navarro, R.: Minimizing artifacts and biases in chamber-based measurements of soil respiration, Agr. Forest Meteorol., 113, 21–37, 2002.

Denmead, O. T. and Bradley, E. F.: On scalar transport in plant canopies, Irrigation Sci., 8, 131–149, 1987.

Dolman, A. J. and Wallace, J. S.: Lagrangian and K-theory approaches in modeling evaporation from sparse canopies, Q. J. Roy. Meteorol. Soc., 117, 1325–1340, 1991.

Ehleringer, J. R. and Osmond, C. B.: Stable isotopes, in: Plant physiological ecology: field methods and instrumentation, edited by: Pearcy, R. W., Ehleringer, J. R., Mooney, H. A., Rundel, P. W., Chapman and Hall, London, 1989.

Farquhar, G. D., Ehleringer, J. R., and Hubick, K. T.: Carbon isotope discrimination and photosynthesis, Annu. Rev. Plant Phy., 40, 503–537, 1989.

Farquhar, G. D., Lloyd, J., Taylor, J. A., Flanagan, L. B., Syvertsen, J. P., Hubick, K. T., Wong, S. C., and Ehleringer, J. R.: Vegetation effects on the isotope composition of oxygen in atmospheric CO_2, Nature, 363, 439–443, 1993.

Farquhar, G. D. and Cernusak, L. A.: On the isotopic composition of leaf water in the non-steady state, Funct. Plant Biol., 32, 293–303, 2005.

Flanagan, L. B., Brooks, J. R., Varney, G. T., and Ehleringer, J. R.: Discrimination against $C^{18}O^{16}O$ during photosynthesis and the oxygen isotope ratio of respired CO_2 in boreal forest ecosystems, Global Biogeochem. Cy., 11, 83–98, 1997.

Flanagan, L. B., Kubien, D., and Ehleringer, J. R.: Spatial and temporal variation in the carbon and oxygen stable isotope ratio of respired CO_2 in a boreal forest ecosystem, Tellus B, 51, 367–384, 1999.

Gillon, J. and Yakir, D.: Influence of carbonic anhydrase activity in terrestrial vegetation on the ^{18}O content of atmospheric CO_2, Science, 291, 2584–2587, 2001.

Griffis, T. J., Baker, J. M., Sargent, S. D., Tanner, B. D., and Zhang, J.: Measuring field-scale isotopic CO_2 fluxes with tunable diode laser absorption spectroscopy and micrometeorological techniques, Agr. Forest Meteorol., 124, 15–29, 2004.

Griffis, T. J., Lee, X., Baker, J. M., Sargent, S. D., and King, J. Y.: Feasibility of quantifying ecosystem-atmosphere $C^{18}O^{16}O$ exchange using laser spectroscopy and the flux-gradient method, Agr. Forest Meteorol., 135, 44–60, 2005a.

Griffis, T. J., Baker, J. M., and Zhang, J.: Seasonal dynamics and partitioning of isotopic CO_2 exchange in C_3/C_4 managed ecosystem, Agr. Forest Meteorol., 132, 1–19, 2005b.

Griffis, T. J., Zhang, J., Baker, J. M., Kljun, N., and Billmark, K.: Determining carbon isotope signatures from micrometeorological measurements: implications for studying biosphere-atmosphere exchange processes, Bound.-Lay. Meteorol., 123, 295–316, 2007.

Griffis, T. J., Sargent, S. D., Baker, J. M., Lee, X., Tanner, B. D., Greene, J., Swiatek, E., and Billmark, K.: Direct measurement of biosphere-atmosphere isotopic CO_2 exchange using the eddy covariance technique, J. Geophys. Res.-Atmos, 113, D08304, doi:10.1029/2007JD009297, 2008.

Griffis, T. J., Sargent, S. D., Lee, X., Baker, J. M., Greene, J., Erickson, M., Zhang, X., Billmark, K., Schultz, N., Xiao, W., and Hu, N.: Determining the oxygen isotope composition of evapotranspiration using eddy covariance, Bound.-Lay. Meteorol., 137, 307–326, 2010.

Haverd, V., Leuning, R., Griffith, D., Van Gorsel, E., and Cuntz, M.: The turbulent Lagrangian time scale in forest canopies constrained by fluxes, concentrations and source distributions, Bound.-Lay. Meteorol., 130, 209–228, 2009.

Kammer, A., Tuzson, B., Emmenegger, L., Knohl, A., Mohn, J., and Hagedorn, F.: Application of a quantum cascade laser-based spectrometer in a closed chamber system for real-time δ^{13}C and δ^{18}O measurements of soil-respired CO_2, Agr. Forest Meteorol., 151, 2011.

Keeling, C. D.: The concentration and isotopic abundances of atmospheric carbon dioxide in rural areas, Geochim Cosmochim. Ac., 13, 322–334, 1958.

Law, B. E., Ryan, M. G., and Anthoni, P. M.: Seasonal and annual respiration of a Ponderosa Pine ecosystem, Glob. Change Biol., 5, 169–182, 1999.

Lee, X. H., Fuentes, J. D., Staebler, R. M., and Neumann, H. H.: Long-term observation of the atmospheric exchange of CO_2 with a temperate deciduous forest in Southern Ontario, Canada, J. Geophys. Res.-Atmos, 104, 15975–15984, 1999.

Lee, X. H., Sargent, S., Smith, R., and Tanner, B.: In situ measurement of the water vapor ^{18}O/^{16}O isotope ratio for atmospheric and ecological applications, J. Atmos Tech., 22, 555–565, 2005.

Leuning, R.: Estimation of scalar source/sink distributions in plant canopies using Lagrangian dispersion analysis: corrections for atmospheric stability and comparison with a multilayer canopy model, Bound.-Lay. Meteorol., 96, 293–314, 2000.

Leuning, R., Denmead, O. T., Miyata, A., and Kim, J.: Source/sink distributions of heat, water vapour, carbon dioxide and methane in a rice canopy estimated using Lagrangian dispersion analysis, Agr. Forest Meteorol., 104, 233–249, 2000.

Miller, J. B., Yakir, D., White, J. W. C., and Tans, P. P.: Measurement of ^{18}O/^{16}O in the soil-atmosphere CO_2 flux, Global Biogeochem. Cy., 13, 761–774, 1999.

Moldrup, P., Olesen, T., Komatsu, T., Yoshikawa, S., Schjonning, P., and Rolston, D. E.: Modeling diffusion and reaction in soils: X. A unifying model for solute and gas diffusivity in unsaturated soil, Soil Sci., 168, 321–337, 2003.

Neumann, H. H. and den Hartog, G.: Leaf-area measurements based on hemispheric photographs and leaf-litter collection in a deciduous forest during autumn leaf-fall, Agr. Forest Meteorol., 45, 325–345, 1989.

Ogée, J., Peylin, P., Cuntz, M., Bariac, T., Brunet, Y., Berbigier, P., Richard, P., and Ciais, P.: Partitioning net ecosystem carbon exchange into net assimilation and respiration with canopy-scale isotopic measurements: an error propagation analysis with $^{13}CO_2$ and $CO^{18}O$ data, Global Biogeochem. Cy., 18, GB2019, doi:10.1029/2003GB002166, 2004.

Ohkubo, S., Kosugi, Y., Takanashi, S., Mitani, T., and Tani, M.: Comparison of the eddy covariance and automated closed chamber methods for evaluating nocturnal CO_2 exchange in a Japanese Cypress forest, Agr. Forest Meteorol., 142, 50–65, 2007.

Pataki, D. E., Ehleringer, J. R., Flanagan, L. B., Yakir, D., Bowling, D. R., Still, C. J., Buchmann, N., Kaplan, J. O., and Berry, J. A.: The application and interpretation of Keeling plots in terrestrial carbon cycle research, Global Biogeochem. Cy., 17, doi:10.1029/2001GB001850, 2003.

Powers, H. H., Hunt, J. E., Hanson, D. T., and Mcdowell, N. G.: A dynamic soil chamber system coupled with a tunable diode laser for online measurements of $\delta^{13}C$, $\delta^{18}O$, and efflux rate of soil-respired CO_2, Rapid Commun. Mass Sp., 24, 243–253, 2010.

Qiu, G. and Warland, J.S.: Inferring profiles of energy fluxes within a soybean canopy using Lagrangian analysis, Agric. For. Meteorol., 139, 119–137, 2006.

Raupach, M.R .: A Lagrangian analysis of scalar transfer in vegetation canopies, Q. J. Roy. Meteorol. Soc., 113, 107–120, 1987.

Raupach, M. R.: A practical Lagrangian method for relating scalar concentrations to source distributions in vegetation canopies, Quart. J. Roy. Meteor. Soc., 115, 609–632, 1989a.

Raupach, M.R.: Applying Lagrangian fluid-mechanics to infer scalar source distributions from concentration profiles in plant canopies, Agric. For. Meteorol., 47, 85–108, 1989b.

Riley, W. J., Still, C. J., Helliker, B. R., Ribas-Carbo, M., and Berry, J. A.: ^{18}O composition of CO_2 and H_2O ecosystem pools and fluxes in a tallgrass prairie: simulations and comparisons to measurements, Glob. Change Biol., 9, 1567–1581, 2003.

Riley, W. J.: A modeling study of the impact of the $\delta^{18}O$ value of near-surface soil water on the delta ^{18}O value of the soil-surface CO_2 flux, Geochim. Cosmochim. Ac., 69, 1939–1946, 2005.

Rochette, P., Flanagan, L. B., and Gregorich, E. G.: Separating soil respiration into plant and soil components using analyses of the natural abundance of carbon-13, Soil Sci. Soc. Am. J., 63, 1207–1213, 1999.

Santos, E. A., Wagner-Riddle, C., Warland, J. S., and Brown, S.: Applying a lagrangian dispersion analysis to infer carbon dioxide and latent heat fluxes in a corn canopy, Agr. Forest Meteorol., 151, 620–632, 2011.

Saxton, K. E. and Willey, P. H.: The SPAW model for agricultural field and pond hydrologic simulation, in: Watershed models, edited by: Frevert, D. K. and Singh, V. P., 2006.

Seibt, U., Wingate, L., Lloyd, J., and Berry, J. A.: Diurnally variable $\delta^{18}O$ signatures of soil CO_2 fluxes indicate carbonic anhydrase activity in a forest soil, J. Geophys. Res.-Biogeo., 111, G04005, doi:10.1029/2006JG000177, 2006.

Skirrow, G.: The dissolved gases: carbon dioxide, in: Chemical Oceanography, edited by: Riley, J. P. and Skirrow, G., Academic Press, San Diego, CA, 1975.

Styles, J. M., Raupach, M. R., Farquhar, G. D., Kolle, O., Lawton, K. A., Brand, W. A., Werner, R. A., Jordan, A., Schulze, E. D., Shibistova, O., and Lloyd, J.: Soil and canopy CO_2, $^{13}CO_2$, H_2O and sensible heat flux partitions in a forest canopy inferred from concentration measurements, Tellus B., 54, 655–676, 2002.

Tans, P. P., Berry, J. A., and Keeling, R. F.: Oceanic C-13/C-12 Observations – a New Window on Ocean CO_2 Uptake, Global Biogeochem. Cy., 7, 353–368, 1993.

Tans, P. P.: Oxygen isotopic equilibrium between carbon dioxide and water in soils., Tellus B, 50, 163–178 , 1998.

Taylor, G.: Diffusion by continuous movements, Proceedings London Mathematical Society, 20, 196–211, 1921.

Teklemariam, T., Staebler, R. M., and Barr, A. G.: Eight years of carbon dioxide exchange above a mixed forest at Borden, Ontario, Agr. Forest Meteorol., 149, 2040–2053, 2009.

Tuzson, B., Mohn, J., Zeeman, M. J., Werner, R. A., Eugster, W., Zahniser, M. S., Nelson, D. D., Mcmanus, J. B., and Emmenegger, L.: High precision and continuous field measurements of $\delta^{13}C$ and $\delta^{18}O$ in carbon dioxide with a cryogen-free QCLAS, Appl. Phys. B-Lasers O., 92, 451–458, 2008.

Wagner-Riddle, C., Thurtell, G. W., and Edwards, G. C.: Trace gas concentration measurements for micrometeorological flux quantification, in: Micrometerology in agricultural systems. Agronomy Monography, edited by: Hatfield, J. L., Baker, J. M., AASA, CSSA, SSSA, Madson, WI, USA., 2005.

Warland, J. S. and Thurtell, G. W.: A Lagrangian solution to the relationship between a distributed source and concentration profile, Bound.-Layer Meteorol., 96, 453–471, 2000.

Weiss, R. F.: Carbon dioxide in water and seawater: the solubility of a non-ideal gas, Mar. Chem., 2, 203–215, 1974.

Welp, L. R., Lee, X., Kim, K., Griffis, T. J., Billmark, K. A., and Baker, J. M.: $\delta^{18}O$ of water vapour, evapotranspiration and the sites of leaf water evaporation in a soybean canopy, Plant Cell Environ., 31, 1214–1228, 2008.

Wilson, J. D.: Turbulent transport within the plant canopy, in: Estimation of areal evapotranspiration, edited by: Black, T. A., Spittlehouse, D. L., Novak, M. D., and Price, D. T., IAHS Publication 177, Wallingford, U.K., 1989.

Wingate, L., Seibt, U., Maseyk, K., Ogee, J., Almeida, P., Yakir, D., Pereira, J. S., and Mencuccini, M.: Evaporation and carbonic anhydrase activity recorded in oxygen isotope signatures of net CO_2 fluxes from a Mediterranean soil, Glob. Change Biol., 14, 2178–2193, 2008.

Wingate, L., Ogee, J., Cuntz, M., Genty, B., Reiter, I., Seibt, U., Yakir, D., Maseyk, K., Pendall, E.G., Barbour, M. M., Mortazavi, B., Burlett, R., Peylin, P., Miller, J., Mencuccini, M., Shim, J. H., Hunt, J., and Grace, J.: The impact of soil microorganisms on the global budget of $\delta^{18}O$ in atmospheric CO_2, Proc. Natl. Acad. of Sci., 106, 22411–22415, 2009.

Wingate, L., Ogee, J., Burlett, R., and Bosc, A.: Strong seasonal disequilibrium measured between the oxygen isotope signals of leaf and soil CO_2 exchange, Glob. Change Biol., 16, 3048–3064, 2010.

Wu, A., Black, A., Verseghy, D. L., and Bailey, W. G.: Comparison of Two-Layer and Single-Layer Canopy Models With Lagrangian and K-Theory Approaches in Modelling Evaporation From Forests, Int. J. Climatol., 21, 1821–1839, 2001.

Xiao, W., Lee, X., Griffis, T. J., Kim, K., Welp, L.R., and Yu, Q.: A modeling investigation of canopy-air oxygen isotopic exchange of water vapor and carbon dioxide in a soybean field, J. Geophys. Res.-Biogeo., 115, G01004, doi:10.1029/2009JG001163, 2010.

Yakir, D. and Wang, X. F.: Fluxes of CO_2 and water between terrestrial vegetation and the atmosphere estimated from isotope measurements, Nature, 380, 515–517, 1996.

Yakir, D. and Sternberg, L. D. L.: The use of stable isotopes to study ecosystem gas exchange, Oecologia, 123, 297–311, 2000.

Zhang, J., Griffis, T. J., and Baker, J. M.: Using continuous stable isotope measurements to partition net ecosystem CO_2 exchange, Plant Cell Environ., 29, 483–496, 2006.

Zobitz, J. M., Keener, J. P., Schnyder, H., and Bowling, D. R.: Sensitivity analysis and quantification of uncertainty for isotopic mixing relationships in carbon cycle research, Agr. Forest Meteorol., 136, 56–75, 2006.